

Multiparametric analysis and validation in the western Mediterranean of three global OGCM hindcasts

ENRIQUE VIDAL-VIJANDE¹, ANANDA PASCUAL¹, BERNARD BARNIER²,
JEAN-MARC MOLINES², NICOLAS FERRY³ and JOAQUÍN TINTORE¹

¹ IMEDEA (CSIC-UIB), Department of Marine Technologies, Operational Oceanography and Sustainability (TMOOS), Carrer Miquel Marquès 21, 07190 Esporles, Spain. E-mail: evidalphoto@gmail.com

² Laboratoire des Écoulements Géophysiques et Industriels, UMR 5519, CNRS, Université Joseph Fourier, Grenoble, France.

³ Mercator Océan, Parc Technologique du Canal, 8-10 rue Hermès, 31520 Ramonville Saint-Agne, France.

SUMMARY: We analyse a hierarchy of three 1/4° global numerical simulations (ORCA-025.G70 (G70), ORCA-025.G85 (G85) and GLORYS1V1 (GLORYS)) by assessing their performance against observational data in the western Mediterranean. When compared with the EN3_v2a temperature and salinity database, the simulations are capable of reproducing surface layer temperature interannual variability but G70 is inaccurate with intermediate and deep-layer trends. This aspect is improved by the increased vertical resolution of G85 and by data assimilation in GLORYS. Salinity is the most problematic parameter because of the imbalance of the freshwater budget derived from inaccuracies in the atmospheric forcing parameters. Surface salinity restoring is needed in order to avoid salinity drift and inaccurate sea-level trends. G70, with a stronger relaxation, has a lower trend closer to altimetric measurements than G85. Mean surface circulation is well reproduced for relatively large-scale signals. We further show that G85 and GLORYS provide evidence of the 2004-2005 and 2005-2006 deep convection events in the Gulf of Lion. Finally, transports through the main straits of the western Mediterranean are correct in order of magnitude, direction and seasonal cycle when compared with observations. This study contributes to the improvement of the ORCA hierarchy of simulations and points out the strengths and weaknesses of these simulations in the Mediterranean Sea.

Keywords: sea level, altimetry, temperature, salinity, modelling, deep-water formation, transports, circulation, Mediterranean Sea.

RESUMEN: ANÁLISIS MULTIPARAMÉTRICO Y VALIDACIÓN DE TRES SIMULACIONES GLOBALES EN EL MEDITERRÁNEO OCCIDENTAL. – Analizamos un conjunto de tres simulaciones numéricas globales de 1/4° (ORCA-025.G70 (G70), ORCA-025.G85 (G85) y GLORYS1V1 (GLORYS)) comparándolas con datos observacionales en el Mediterráneo Occidental (WMED). Contrastando con la base de datos de temperatura y salinidad EN3_v2a las simulaciones son capaces de reproducir la variabilidad superficial en temperatura sin embargo G70 exagera las tendencias en capas intermedias y profundas. Este aspecto es mejorado por la mayor resolución vertical de G85 y la asimilación de datos de GLORYS. La salinidad es el parámetro más problemático debido al desequilibrio del balance de agua dulce procedente de imprecisiones en los parámetros de forzamiento atmosférico. Relajación de salinidad superficial es necesaria para evitar derivas de salinidad y nivel del mar. De hecho G70 con su relajación más intensa tiene una tendencia más baja (y más cercana a mediciones altimétricas) que G85. La circulación promedio en superficie está bien reproducida para señales relativamente grandes. Además, demostramos que G85 y GLORYS muestran evidencia de los eventos de convección profunda de 2004-2005 y 2005-2006 en el Golfo de León. Finalmente, transportes a través de los principales canales y estrechos del Mediterráneo Occidental son correctos cuando se comparan con observaciones, tanto en orden de magnitud y dirección, como en el ciclo estacional. Este estudio contribuye a la mejora del conjunto de simulaciones ORCA y señala las fortalezas y debilidades de estas simulaciones en el Mar Mediterráneo.

Palabras clave: nivel del mar, altimetría, temperatura, salinidad, modelos numéricos, formación de aguas profundas, transportes, circulación, mar Mediterráneo.

INTRODUCTION

Long-term ocean variability has traditionally been studied using in situ observational records. However, due to their often sparse spatial and temporal resolution these records do not provide a complete picture of ocean variability. With the advent of satellite observations, global coverage of surface ocean processes has improved considerably, but these observations have only been available for the last ~20 years and cannot provide information of the entire water column. Recent numerical hindcast simulations, on the other hand, provide the continuous and complete evolution of the ocean for the simulation period but require careful quantitative assessments and model-observation mismatch evaluations to guide dynamical studies and further model improvements (Penduff *et al.* 2007).

Because of computational limitations, ocean models must compromise their configurations in terms of resolution, area covered, equation approximations/simplification and other parameterizations (Kantha and Clayson 2000). In order to study three-dimensional ocean variability, the models must be baroclinic, global or regional, have sufficient resolution to resolve the features to be studied, maintain a free-surface formulation (if sea level and mass addition are features to be studied) and be coupled to the atmosphere via either external atmospheric forcing or coupled atmospheric models. One of the typical simplifications used in large-scale ocean circulation models is the hydrostatic/Boussinesq approximation. This ignores density changes in the fluid except when gravitational forces are involved. This simplification is appropriate for modelling horizontal features greater than 10 km (10-1000 km going from mesoscale eddies to oceanic gyres) because below this resolution the hydrostatic approximation does not hold.

Resolution is another key parameter that defines the performance of an ocean model at various scales. Higher resolution is always preferable although it is limited by computational and storage capabilities. This is why regional models are capable of operating at higher resolution than global models and are thus preferred for regional studies. Several regional modelling studies have focused on the Mediterranean Sea using high-resolution 1/8° and 1/16° regional models such as DieCAST (Fernández *et al.* 2005), OPAMED8 (Somot *et al.* 2006), EU-MFSTEP (Tonani *et al.* 2008) NEMOMED8 (Sevault *et al.* 2009) and MED16 (Beranger *et al.* 2010) to name a few. The DieCAST 1/8° simulation used in (Fernández *et al.* 2005) is not a hindcast but rather a simulation run to assess circulation and transport variability in the Mediterranean Sea. It is forced by climatological monthly mean winds and uses relaxation towards monthly climatological surface temperature and salinity. The OPAMED8 1/8° simulation by Somot *et al.* (2006) is a scenario of the Mediterranean Sea under climate change IPCC-A2 conditions run with an atmospheric regional climate model (AR-

PEGE) over the 1960-2099 period using a hierarchy of three different models. The objective of these models is to obtain a high-resolution atmospheric forcing to run the OPAMED8 simulation (based on the OPA model (Madec *et al.* 1998) of the Mediterranean Sea under a transient climate change scenario. The EU-MFSTEP 1/16° simulation by Tonani *et al.* (2008) is a very high resolution model based on the OPA code (Madec *et al.* 1998) and used for operational daily forecasts of the Mediterranean Sea. It has been available since 1997. The NEMOMED8 1/8° simulation by Sevault *et al.* (2009) is a simulation focusing on the study of the dynamics behind certain features and variability of the Mediterranean Sea, which has also been used in the recent studies by Beuvier *et al.* (2010) and Herrmann *et al.* (2010) that focused on the EMT and the 2005-2006 NW Mediterranean convection events, respectively. The MED16 (Beranger *et al.* 2010) is a modelling experiment to assess the performance of atmospheric forcing resolution on winter ocean convection in the Mediterranean Sea by running two 4-year simulations 1998-2002 (with 11-year spin-up), one using ERA40 and one using surface fields analysed by the European Centre for Medium-Range Weather Forecasts (EC-MWF) that have twice the resolution of ERA40.

However, regional models are not without their own problems; these models require that their boundary conditions be provided either by nesting into a coarser-resolution model or through relaxation to climatology. Nesting within a coarser-resolution model can introduce errors due to differences in the parameterization of the physical processes in the two models and errors due to the numerical techniques used for the nesting, which can propagate these errors into the regional domain, having a significant impact on the simulation's evolution (Calafat 2010).

Few studies have focused on the performance of global ocean models in the western Mediterranean Sea (Tsimplis *et al.* 2008, 2009). One such study performed by Vidal-Vijande *et al.* (2011) conducted an assessment of the global ocean model ORCA025-G70 in the Mediterranean Sea against satellite and hydrographic data. It is in this context that we propose to expand on Vidal-Vijande *et al.* (2011) and perform the validation in the Mediterranean Sea of a series of 1/4° global ocean simulations based on the NEMO code (Madec 2008): two climatic scale hindcasts, ORCA025 G70 (G70 hereafter) and ORCA025 L75.G85 (G85 hereafter); and one shorter simulation with data assimilation, GLORYS1V1 (hereafter GLORYS). The inclusion of GLORYS reanalysis in this study is aimed at verifying that reanalysis products that include data assimilation help to improve the description and our understanding of ocean variability in the western Mediterranean Sea (WMED). It will highlight the degree of improvement that can be expected from an ocean reanalysis in this region in comparison with a free run.

This study will focus primarily on the WMED (Fig. 1). After carrying out a general assessment of tempera-

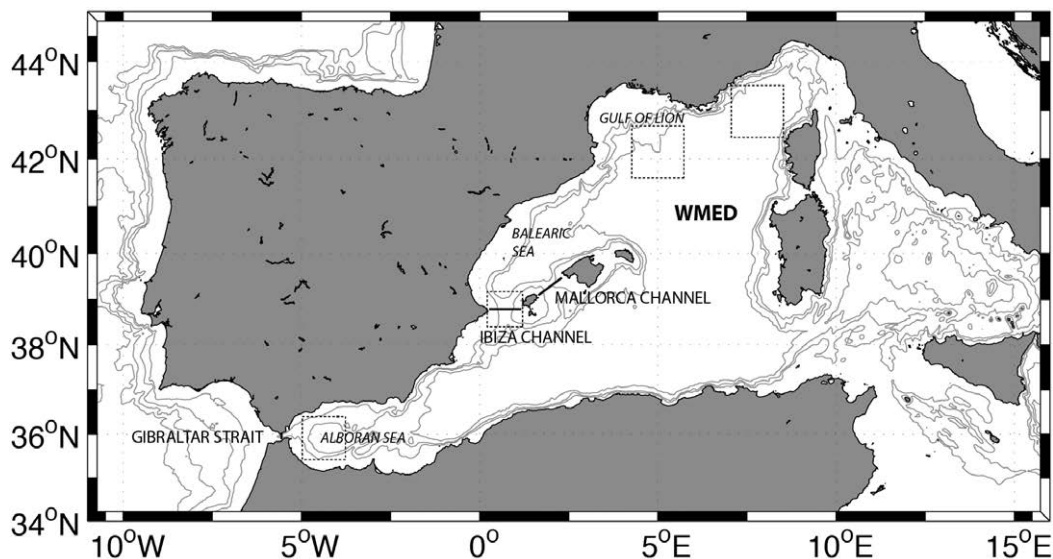


FIG. 1. – Map of the western Mediterranean (WMED) showing the straits and channels studied and the areas used to create Hovmöller diagrams. Isobaths of 500, 1000, 2000 and 3000 metres are also shown.

ture and salinity, particular attention will be paid to the models' capability to reproduce the deep water formation in the Gulf of Lions and its transport through the Balearic Sea. The basin average sea-level trends will be compared against satellite altimetry and the mean circulation evaluated with two different mean dynamic topographies. The transport at Gibraltar and the exchanges at the Balearic Channels, Mallorca and Ibiza, where most of the WMED north-south exchanges of heat and water take place (Pinot *et al.* 2002), will also be analysed.

DATA

The ORCA Simulations (G70 and G85)

In this study we analyse the ORCA-R025 G70 and ORCA-R025 L75.G85 numerical simulations (G70 and G85 hereafter) developed by the DRAKKAR Group (Barnier *et al.* 2006), which are aimed at studying ocean variability under realistic atmospheric conditions (from ECMWF/ERA40 [Simmons and Gibson 2000]) over the last 50 years (1958-2007).

Both models simulate the evolution of temperature, salinity, velocity, sea surface height (SSH), sea-ice characteristics, and oceanic concentrations of tracers (CFC11 and C14) (Barnier *et al.* 2007). Both use a global configuration of NEMO (Madec 2008) implemented on a $1/4^\circ$ resolution grid. Effective resolution becomes finer with increasing latitudes (in this case ~ 27.75 km at the equator, ~ 21.8 km in the Mediterranean and ~ 13.8 at 60°N/S). At this resolution, the simulations are eddy-permitting but not eddy-resolving in large oceans such as the Atlantic, but they are not eddy-permitting in the Mediterranean, where the first Rossby radius of deformation is around 10 to 15 km (Lebeaupin *et al.* 2011). Grid, masking, and initial

conditions are inherited from the global configuration of the MERCATOR Océan operational oceanography centre, with 1442×1021 grid points and 46 vertical levels for G70 and 75 vertical levels for G85. Vertical grid spacing is finer near the surface and increases with depth (maximum depth is 5844 m).

Bathymetry is derived from the 2-min-resolution Etopo2 bathymetry file of the NOAA National Geophysical Data Centre. Some smoothing is applied when the bathymetry is added (including the Gibraltar Strait, where the strait was widened to allow suitable flow given the coarse resolution of the model). Initial conditions for temperature and salinity were derived from the NODC World Ocean Atlas data set for middle and low latitudes. For the Mediterranean, initial conditions were derived from the MEDAR climatology (more details can be found in Barnier *et al.* [2006]) and Molines *et al.* [2007]). Atmospheric forcing for both models is a hybrid forcing based on the ECMWF/ERA40 reanalysis (~ 125 km resolution) and CORE (Large and Yeager 2004). In the case of G70 the forcing used is the DFS3 (DRAKKAR Forcing Set 3), which is based on un-corrected surface atmospheric state variables of ERA40 extended in time until 2007 with fields of the ECMWF operational analysis and the radiation and precipitation products of CORE. This forcing is globally imbalanced for heat ($+12.8 \text{ W m}^{-2}$) and freshwater ($+56 \text{ mm/year}$). G85 is forced with the DFS4, which is an improved version of DFS3 with corrections applied to ECMWF variables (air temperature, air humidity, wind speed) to remove unrealistic time discontinuities (induced by changes in the nature of assimilated observations, especially in 1979 when satellite data began to be assimilated) and obvious global and regional biases in ERA40 fields (in comparison with high-quality observations). Corrections also aimed to improve continuity between ERA40 and ECMWF operational analyses

in 2002. Wind speed corrections consist in rescaling ERA40 and ECMWF winds with 6 years of QSCAT scatterometer winds. The result for the Mediterranean Sea is that wind speeds are increased by about 10% in DFS4. Finally, the CORE radiation and precipitation fields were submitted to a small adjustment (in zonal mean) that yields a near-zero global imbalance of heat ($+0.3 \text{ W m}^{-2}$) and freshwater (-0.2 mm yr^{-1}). Detailed information on ERA40, DFS3 and DFS4 can be found in Brodeau *et al.* (2009).

Since these simulations do not achieve freshwater balance, and to avoid and prevent an unacceptable drift in the model, a sea surface salinity (SSS) restoring term was applied at the surface. This term attempts to balance the freshwater budget by restoring SSS to climatology (adding evaporation or precipitation where necessary). This restoring term tends to adversely affect the simulation's interannual variability. In G85 the SSS relaxation is 1/6th that of G70.

The GLORYS1V1 simulation with data assimilation

GLORYS1V1 (hereafter GLORYS) is the first of a number of simulations created by the French Global Ocean Reanalysis and Simulations framework and is based on the PSY3V2 operational system used at Mercator. It is also a global implementation of the NEMO framework and shares many features with the ORCA-025 simulations described above (particularly G70 with the same forcing and sea-ice model). The simulation spans the "Argo" era from 2002-2008 and uses data assimilation from a variety of sources, including sea surface temperature (SST) maps, along-track sea-level anomaly (AVISO delayed mode) and in situ temperature and salinity profiles from the CORA-2 and CORIOLIS databases. The model does not perform any relaxation in SST or SSS. The atmospheric forcing consists of daily averages of atmospheric variables provided by ECMWF operational analyses and the CLIO bulk formulation (Goosse *et al.* 2001) is used. The ECMWF precipitation field has been corrected using GPCP monthly data and the model global freshwater balance is constrained to be zero at each time step.

Hydrographic databases

Three different hydrographic datasets were considered to perform the comparison and validation of the simulations. These datasets are the following:

- The MEDAR dataset (MEDAR-Group, hereafter MEDAR) consisting of yearly temperature (T) and salinity (S) fields covering the Mediterranean Sea on a $0.2^\circ \times 0.2^\circ$ horizontal grid and 25 vertical levels spanning the period 1942-2002 (Rixen *et al.* 2005).
- The Ishii dataset (Ishii and Kimoto 2009) (hereafter ISHII), which consists of monthly $1^\circ \times 1^\circ$ gridded global T and S fields spanning the period 1945-2006 and covering from the surface to 700 m.

- The ENACT/ENSEMBLES version 3 (EN3-v2a) dataset (hereafter EN3) (Ingleby and Huddleston 2007) produced by objective analysis of the T and S profiles of the World Ocean Database '05, the Global Temperature and Salinity Profile Project, Argo and the Arctic Synoptic Basin-Wide Oceanography Project. The dataset consists of global monthly T and S fields on a $1^\circ \times 1^\circ$ grid covering the period 1950 to the present. The vertical domain extends down to 5000 m, with data on 42 levels.

Satellite altimetry

Satellite altimetry provides realistic high-resolution SSH observations, making it a useful tool for validating sea-level and surface circulation in numerical models. However, altimeter measurements also include the Earth's geoid, which varies tens of metres across the ocean and needs to be subtracted from altimetry data to obtain a usable product (Dobricic 2005). Because the exact shape of the geoid is largely unknown (the best data available comes from the GRACE satellite measurements with a resolution of approximately 300 km, which is only sufficient for large-scale studies), the typical solution to circumvent this limitation is to subtract a temporal mean of SSH at each location, leaving only the variable components of sea surface height, known as sea-level anomaly.

The altimetry dataset used in this work is the REF MERGED SLA product available through the AVISO FTP (<http://www.aviso.oceanobs.com>). This dataset consists of gridded, delayed-time sea-level anomaly fields specific for the Mediterranean Sea that merge several altimeter missions (Topex/Poseidon, Jason-1, ERS 1/2, ENVISAT). The gridded maps are provided weekly on a $1/8^\circ$ grid and the reference product was selected in order to have a homogeneous time series with the same configuration of satellite altimeters as that included in the objective analysis scheme. For more details on the altimeter data processing the reader is referred to Pujol *et al.* (2005). For this study, monthly means were computed from weekly gridded maps (averaging 4-5 maps for each month).

RESULTS AND DISCUSSION

Temperature

In order to assess the simulations' performance with regard to temperature and salinity, the WMED was divided into vertical layers (Figs 2 and 3) following the previous study by Vidal-Vijande *et al.* (2011), which was in turn based on the method used by Rixen *et al.* (2005). The numerical models were compared with the EN3 hydrographic database. For these comparisons, the simulation data for G70 and G85 and the EN3 hydrographic data were filtered using a one-year running average in order to remove the intra-annual variability and focus on the longer 44- to 47-year pe-

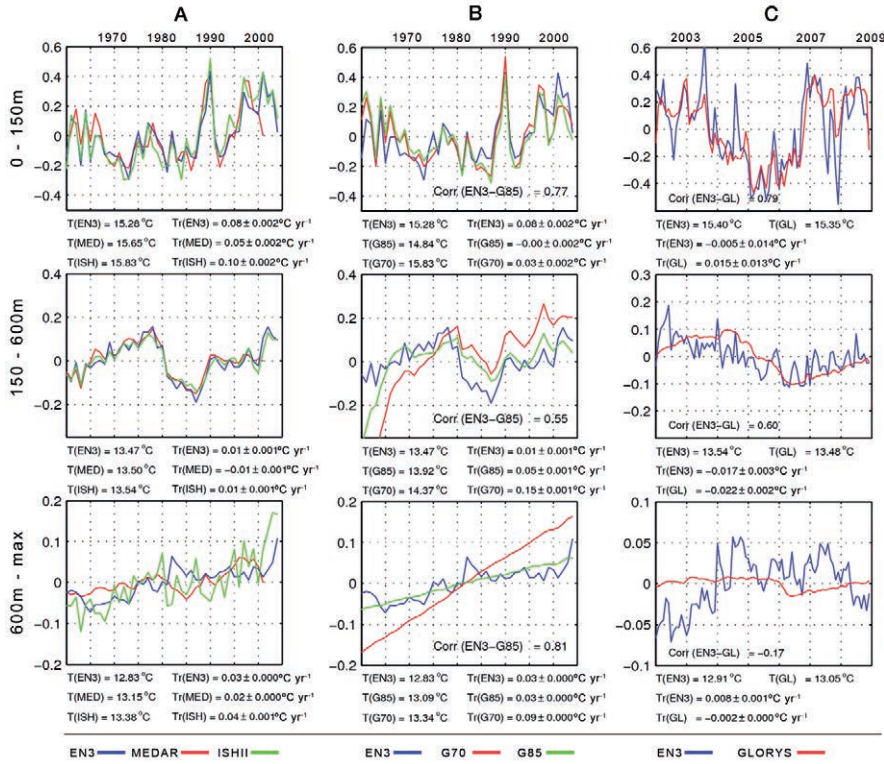


FIG. 2. – WMED mean temperature anomaly of the interannual variability at different layers. A, is the comparison between EN3, MEDAR and ISHII from 1960 to 2004. B, is the comparison between EN3, G70 and G85 from 1960 to 2004. C, is the comparison between EN3 and GLORYS from 2002 to 2009. Mean temperatures (T) and trends (Tr) with their error are given below each image for the data streams. A colour version of this figure may be found in the online electronic manuscript.

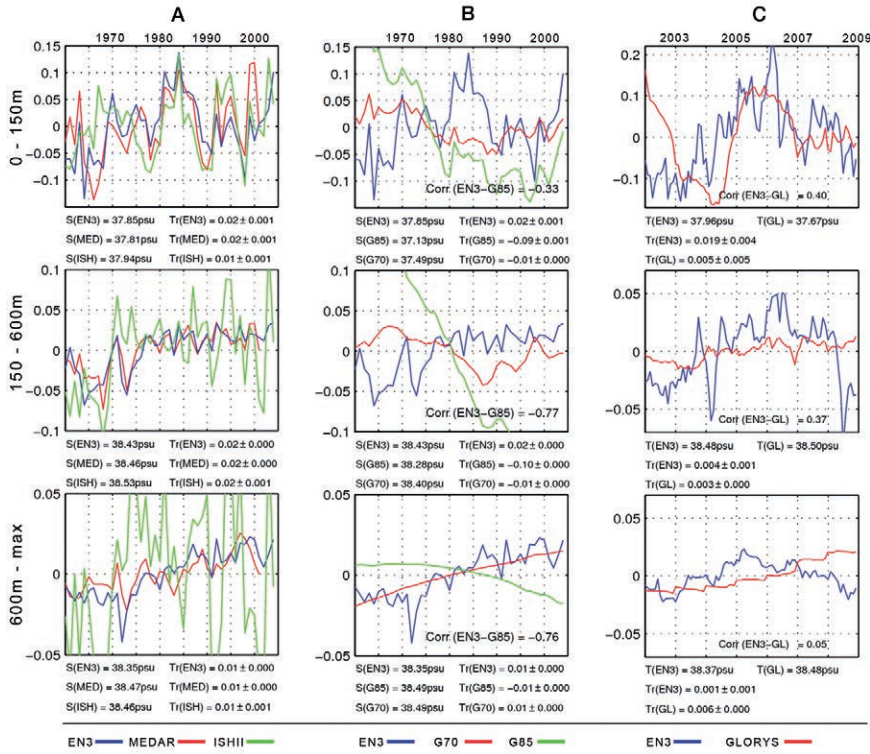


FIG. 3. – WMED mean salinity anomaly of the interannual variability at different layers. A, is the comparison between EN3, MEDAR and ISHII from 1960 to 2004. B, is the comparison between EN3, G70 and G85 from 1960 to 2004. C, is the comparison between EN3 and GLORYS from 2002 to 2009. Mean salinities (S) and trends (Tr) with their error are given below each image for the different data streams. A colour version of this figure may be found in the online electronic manuscript.

riod variability. For GLORYS, because the simulation is much shorter (2002-2009), the data were not filtered annually.

Figure 2 shows the temperature time series averaged over the WMED at different depth layers. Figure 2A is the initial comparison of the three observational datasets (MEDAR, ISHII and EN3). All three datasets behave similarly, except for ISHII at deep layers (because it only reaches 700 m) and for salinity at intermediate and deep layers, where the variability is much higher than that of the other two. Of all three datasets, EN3 was deemed the most appropriate because of its compromise between temporal resolution (monthly), depth range (0-5000 m) and period (1950 to the present).

Figure 2B shows the comparison between EN3, G70 and G85. Both G70 and G85 have near-identical variability at the surface layers, and are in good agreement with EN3. G85 correlates especially well with EN3 (detrended correlation of 0.87). The major difference found between the three datasets at surface layers is a bias in mean temperature. Taking EN3 as the reference, G85 is 0.44°C cooler and G70 is 0.55°C warmer.

At intermediate layers (150-600 m), G70 shows an exaggerated positive trend that is reduced in G85 when compared with EN3 ($G70=0.15^{\circ}\text{C yr}^{-1}$, $G85=0.05^{\circ}\text{C yr}^{-1}$ and $EN3=0.01^{\circ}\text{C yr}^{-1}$) and mean temperature values ($G85=13.92^{\circ}\text{C}$, $EN3=13.47^{\circ}\text{C}$). Deep layers also show significant improvement, with G85 and EN3 showing similar trends and closer mean values (although interannual variability is non-existent in both simulations).

The improvement in temperature trends in G85 can be attributed to two factors: the better time continuity of the DFS4 forcing, which has an impact on long-term trends; and the increased vertical resolution, which has a strong effect on the vertical mixing coefficient of the turbulent closure scheme.

The differences in mean temperatures are also a result of the atmospheric forcing parameters: DFS3 (G70) is globally imbalanced for heat resulting in a warming ocean, hence higher mean temperatures. On the other hand, DFS4 (G85) maintains a near-zero global heat balance. DFS4 also has stronger wind speeds, causing a global cooling of surface waters, which together with the better vertical mixing coefficients because of increased vertical resolution helps to propagate the effects of the atmospheric forcing throughout the water column and to maintain a better correspondence with the observations. However, as will be discussed in the following section, the inability of the model to reproduce winter deep convection in the Gulf of Lions causes temperatures at intermediate and deep layers to increase, showing a positive temperature bias.

As is to be expected from a model with data assimilation, GLORYS performs well when compared with the EN3 observational data. At surface layers, GLORYS has slightly weaker peaks in its interannual variability but the overall pattern of variability is very similar, with high correlations of 0.77 over the WMED. Intermedi-

ate layers also show relatively good performance, with slightly lower correlations of 0.66, although the model shows very low interannual variability, similar to the behaviour of the ORCA models. This might be due to a reduced number of sub-surface observations included in the data assimilation. At deep layers, the basin mean temperature does not show the 2004 spike caused by the production of anomalously warm and salty deep water during the winters of 2004-2005 and 2005-2006 (Schroeder *et al.* 2008b, 2010). However, as seen in Figure 6, the simulation does indeed create a strong convection event in the 2005-2006 winter.

The behaviour of the models in comparison with observations at different frequency bands was also analysed using spectral analysis (not shown). WMED spatially averaged power spectra were computed showing that for the simulations a predominant peak is registered in surface temperature at 10-12 months corresponding to the annual cycle, and the same occurs for EN3. A weaker semi-annual peak at 6 months also appears in the simulations but is not clearly found in the observations.

Salinity

While EN3 salinity trends are always either slightly positive or close to zero, both G85 and G70 simulations show negative trends at surface and intermediate layers, with G85 displaying trends 5 to 8 times stronger than G70. This is because the salinity relaxation that is applied to the G85 simulation is 1/6th of that imposed in G70. This lower relaxation applies less evaporation to the simulation, causing a very strong and unrealistic negative trend in salinity and making the mean values over the period studied much lower (at surface layers, $EN3=37.93$, $G85=37.13$) than those obtained from the EN3 observational data. Consequently, the power spectra of G85 and EN3 are very different (not shown). At deep layers, G70 and EN3 coincide with slight positive trends (~ -0.03 - 0.05 psu yr^{-1}) but G85 remains negative at ~ -0.08 psu yr^{-1} . Caution must be taken when analysing observational salinity data in deep layers as they are very scarce and unevenly spread, and therefore prone to significant averaging error.

Salinity in GLORYS appears slightly better than in the ORCA models but still does not produce good results. At surface layers, the model shows a strong deviation with regard to EN3 (~ 0.25 psu in salinity anomaly in the WMED) towards the beginning of the simulation but manages to stabilize and approximate EN3 by 2005. This deviation during the initial years may be due to the fact that GLORYS uses the ARIVO climatology (Gaillard *et al.* 2008, Gaillard and Charraudeau 2008), which is different from the climatology used in the background field in the EN3 optimal interpolation. Additionally, salinity data in 2002 and 2003 are very scarce, reducing the confidence in the EN3 dataset. Also GLORYS assimilation of observations other than in situ profiles, namely altimetry and SST,

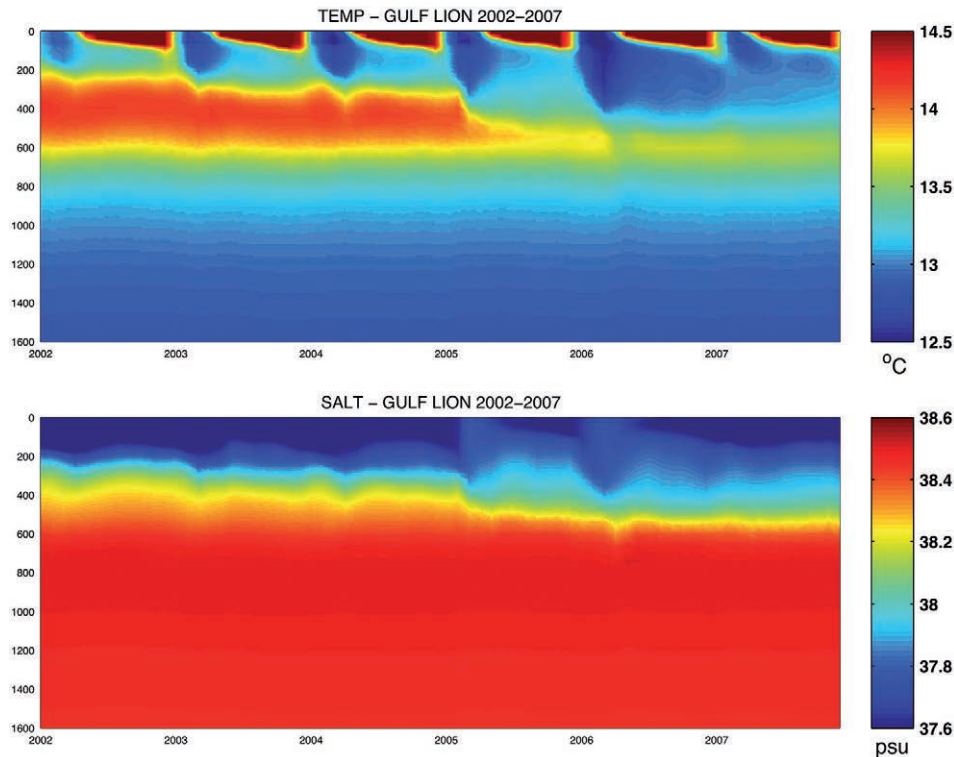


FIG. 4. – Hovmöller diagrams showing the temporal evolution of temperature (top) and salinity (bottom) of a $1^{\circ}\times 1^{\circ}$ area at the centre of the Gulf of Lions for the G85 simulation. A colour version of this figure may be found in the online electronic manuscript.

could be part of the difference (through the use of multivariate covariances). At intermediate and deep layers, GLORYS seems to show a positive drift in salinity with very marked and unrealistic “steps” at the end of each year (especially in deep layers). EN3 displays a significant increase in salinity in deep layers of approximately 0.05, peaking in 2005 and a reduction after that. This behaviour is difficult to explain. This could be related to the 2005-2006 deep convection events that caused an increase in salinity at those depths and were studied by Schroeder *et al.* (2006, 2008a, 2010), Herrmann *et al.* (2010), Font *et al.* (2007) and Smith *et al.* (2008). Another possible explanation is that the peak in EN3 may be due to lack of observations at that depth. This is not observed in the model.

Deep-water formation in the Gulf of Lions and propagation towards the Ibiza Channel

One important issue to be explored is the capability of these models to reproduce deep water formation events. Given the nature of these events, which are caused by localized extreme weather (wind and cold) events, the spatial and temporal resolution of the simulations is a heavily limiting factor, as is the low resolution of the atmospheric forcing. Despite these limitations, in this section we evaluate the interannual variability of deep water using Hovmöller diagrams of mean vertical temperature and salinity profiles from the Gulf of Lions deep water formation sites.

Figure 4 shows the temporal evolution of the vertical temperature and salinity profiles (the mean of a $1^{\circ}\times 1^{\circ}$ centred at 42.6°N , 4.4°E) for G85. Every winter, cold water sinks down through the water column to about 200 to 300 m. For the entire G85 simulation period (1960 to 2007, not shown), the propagation of these colder waters does not seem to go beyond that level, instead stopping as it encounters the Levantine Intermediate Water (LIW). However, the winters of 2004-2005 and 2005-2006 show the propagation of these colder waters penetrating into the intermediate layers and significantly modifying their signature, with the latter producing a thin tongue of colder water reaching beyond 750 m and into the deep layers. As can be seen in Figure 5, which shows the net downward heat flux and the net upward water flux, the winters of 2005 and 2006 also show very intense evaporation and heat loss ($\sim 240 \text{ W m}^{-2}$), setting the appropriate conditions for deep water formation.

One notable difference between EN3 (Fig. 6) and G85 is the warmer intermediate waters (by approximately 0.5°C) in the simulation prior to these two exceptional winters. As is evidenced by the winters of 2004-2005 and 2005-2006, these convection events play an important role in conditioning the temperature of intermediate layers by mixing down colder waters. Given the low resolution of the model, and especially of the atmospheric forcing, weaker deep convection events are not reproduced by the simulation and cause intermediate layers to heat up by diffusion (the initial

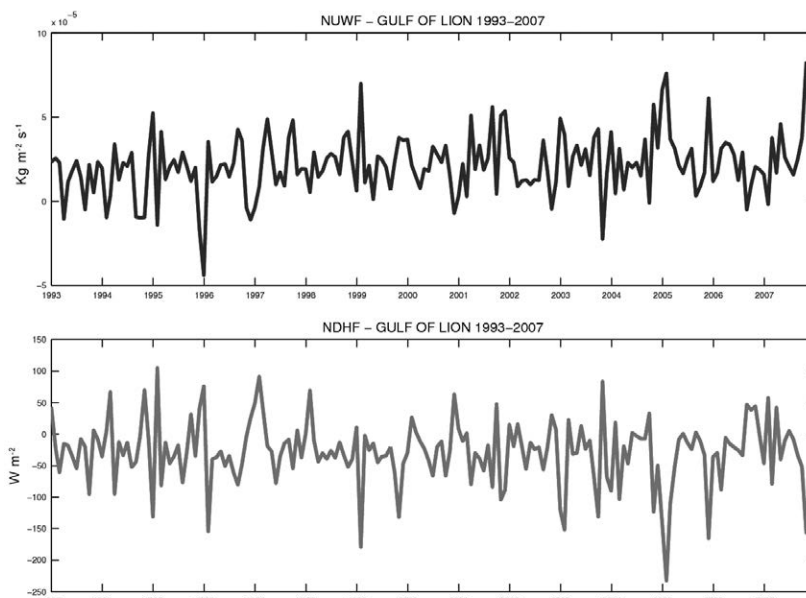


FIG. 5. – Time series plots of net upward water flux (top) and net downward heat flux (bottom) over a $1^{\circ} \times 1^{\circ}$ area of the Gulf of Lions for the G85 simulation.

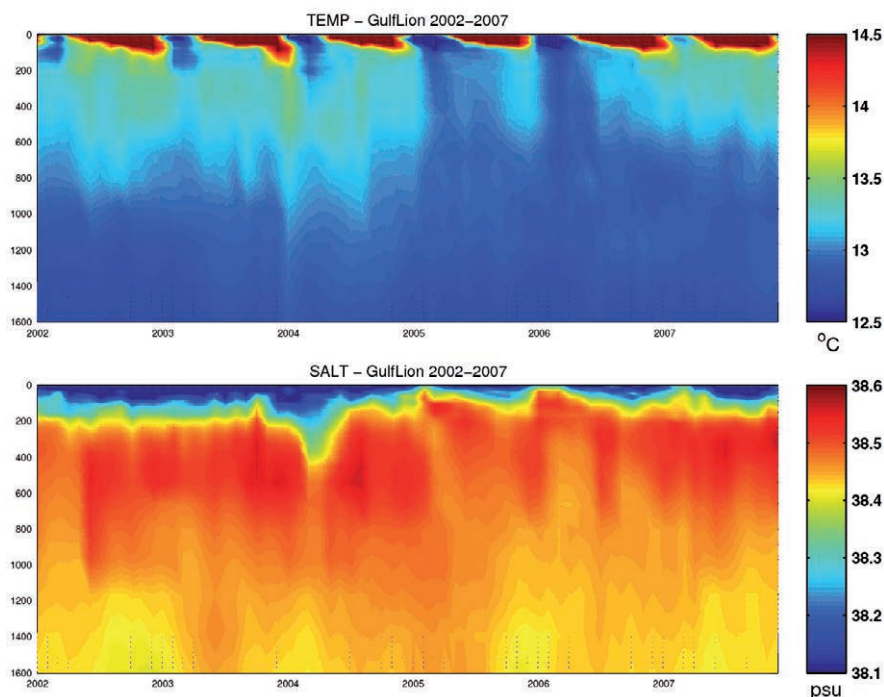


FIG. 6. – Hovmöller diagrams showing the temporal evolution of temperature (top) and salinity (bottom) of a $1^{\circ} \times 1^{\circ}$ area at the centre of the Gulf of Lions for the EN3 database. A colour version of this figure may be found in the online electronic manuscript.

years of the simulation have similar temperatures to the observations but from 1960 to 1965 there is a rapid warming of this layer).

The 2005 and 2006 events are clearly visible in the EN3 dataset (Fig. 6), with both years producing strong convection. These results correspond to the deep water formation events described in Schroeder *et al.* (2006, 2008a, 2010), Herrmann *et al.* (2010), Font *et al.* (2007) and Smith *et al.* (2008) that were produced by

extremely strong forcing during these two winters (heat loss 70% above average according to López-Jurado *et al.* [2005] and low precipitation according to Font *et al.* [2007]). In fact, the ARPERA dataset (Herrmann and Somot 2008), which is a dynamical downscaling of the ERA40 dataset (from 150 to 50 km) gives a net winter heat loss for that area of 308 W m^{-2} for the 2004-2005 winter, whereas other winters show net losses of $\sim 200 \text{ W m}^{-2}$ (Table 1, Schroeder *et al.* 2010).

A similar difference is seen in G85, although the total heat loss is less due to the lower resolution of the ERA40 atmospheric forcing (240 W m^{-2} in 2004-2005 vs $\sim 150 \text{ W m}^{-2}$ during most other winters). The temporal and spatial effects of the atmospheric forcing resolution on deep convection were studied by Beranger *et al.* (2010) using high-resolution ($1/16^\circ$) numerical

simulations and running both ERA40 ($\sim 125 \text{ km}$) and ECMWF ($\sim 55 \text{ km}$) forcing. They concluded that the higher resolution forcing generated the more realistic (and stronger) winds and winter heat loss necessary for the formation of deep convection events.

A similar analysis was performed with GLORYS over the period 2002-2009 (Fig. 7). Daily outputs were

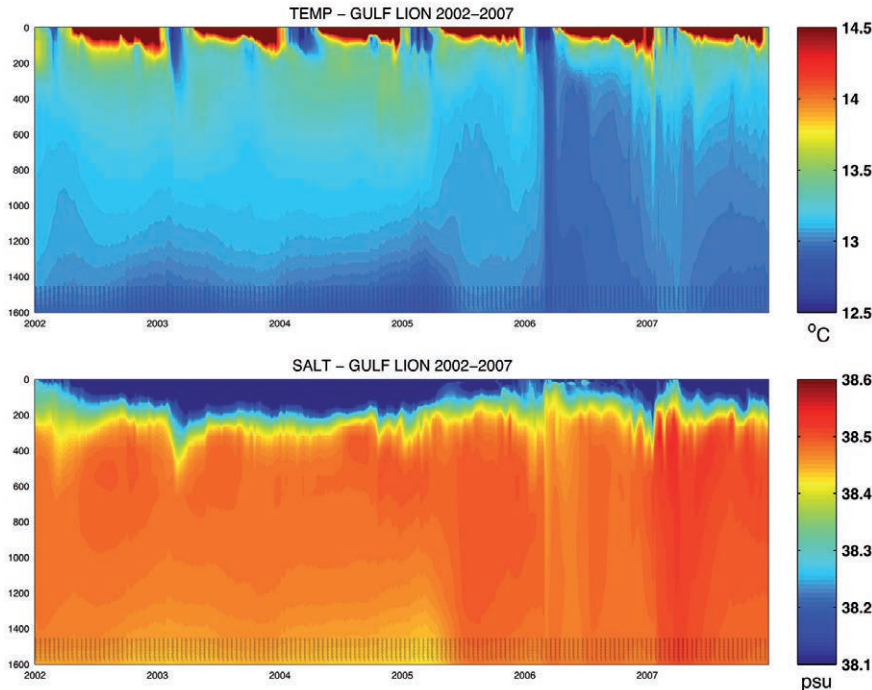


FIG. 7. – Hovmöller diagrams showing the temporal evolution of temperature (top) and salinity (bottom) of a $1^\circ \times 1^\circ$ area at the centre of the Gulf of Lions for the GLORYS simulation. A colour version of this figure may be found in the online electronic manuscript.

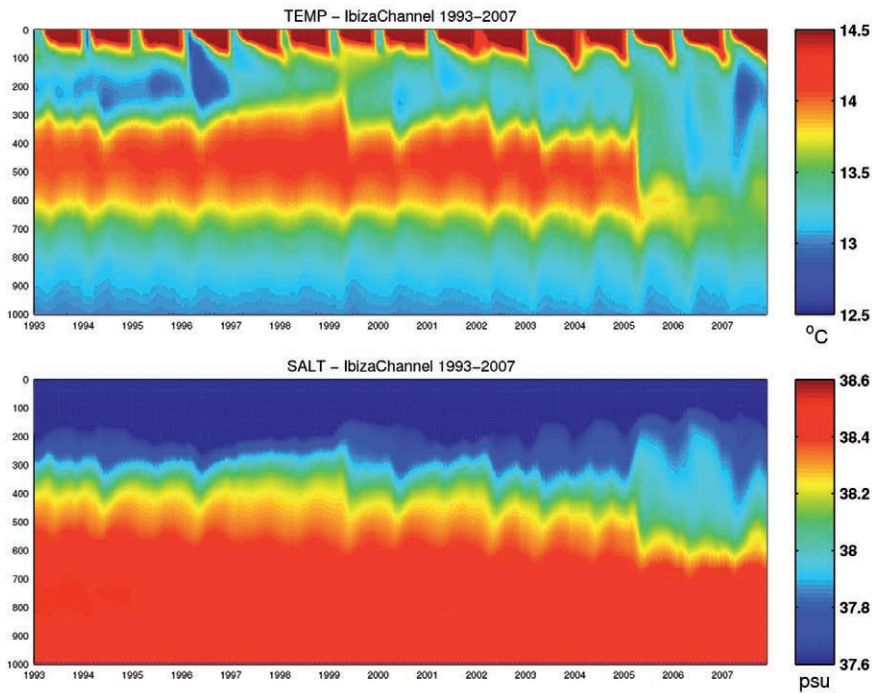


FIG. 8. – Hovmöller diagrams showing the temporal evolution of temperature (top) and salinity (bottom) of a $1^\circ \times 1^\circ$ area at the centre of the Ibiza Channel for the G85 simulation. A colour version of this figure may be found in the online electronic manuscript.

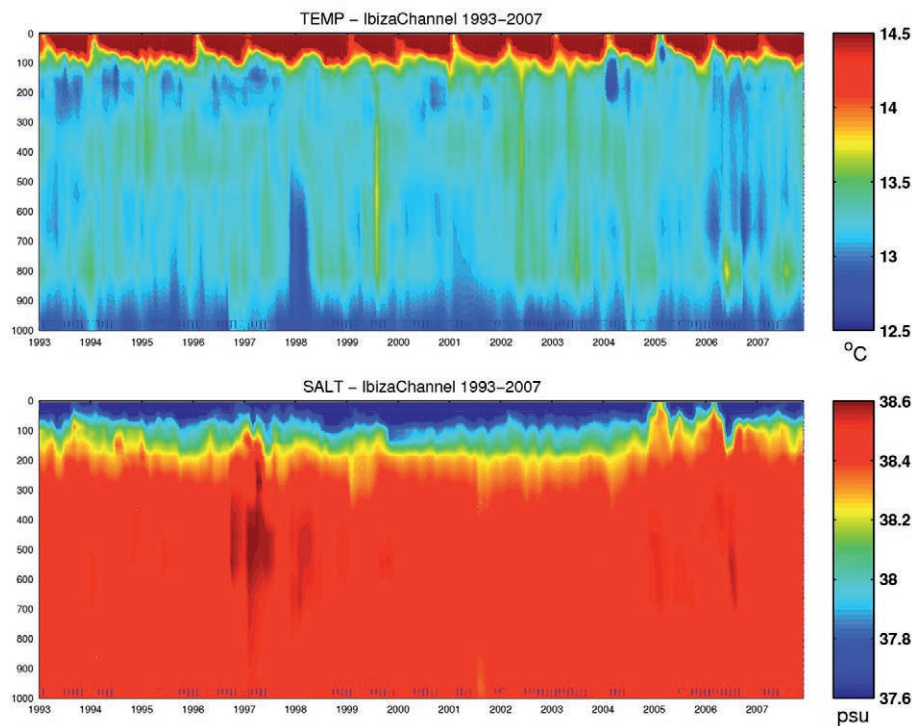


Fig. 9. – Hovmöller diagrams showing the temporal evolution of temperature (top) and salinity (bottom) of a $1^{\circ}\times 1^{\circ}$ area at the centre of the Ibiza Channel for the EN3 data. A colour version of this figure may be found in the online electronic manuscript.

available for this simulation, greatly increasing the temporal resolution, a factor which is very important in these localized deep water formation events. In GLO-RYS the year of most intense cooling was 2006, with a very distinct cooling signal throughout the water column reaching the deep layers and changing the properties of intermediate and deep waters for the following years. However, the 2005 event is weaker than the observations and does not reach beyond the intermediate layers. This disparity between GLO-RYS, which assimilates data, and EN3 could be due to several factors: the ECMWF operational system which provides the ocean-atmosphere fluxes for the simulation increased its resolution from 0.5° to 0.25° in February 2006, just prior to the onset of the deep convection event. This resolution increase would clearly benefit the formation of deep convection events and could partly explain the difference from the previous year. EN3 and the assimilated CORA database may contain different profiles (due to differences in quality control parameters or source data).

Additional tests were performed in different areas of the WMED and similar $1^{\circ}\times 1^{\circ}$ squares were taken in the Ibiza Channel and the Alboran Sea just before the Strait of Gibraltar. In the Ibiza Channel (Fig. 9), similar (but less intense) cooling of the upper and intermediate layers occurs. Figure 10 is a composite of TS diagrams for the years 1996, 1997, 2003 and 2006 in the Ibiza Channel. Presence of LIW and Western Mediterranean Deep Water (WMDW) is clear in all four years but 1996 and 2006 also show a clear presence of Western Mediterranean Intermediate Water (WIW) with temperature minima between 13°C and 12.5°C . The

years 1996 and 1997 were chosen because Pinot *et al.* (2002) performed extensive measurements during the CANALES experiment in the Ibiza and Mallorca channels, which can be readily compared with the simulation data. The 1996 WIW peak in the G85 TS diagram and the temperature minima coincide with Pinot *et al.* (2002), as does the lack of WIW in 1997. At the Alboran site, the effects of these two winters are far weaker, but the modification of intermediate waters seems to reach this location by mid-2006.

These deep water formation events were reproduced to some extent because of the extremity of the atmospheric forcing. Li *et al.* (2006) and Herrmann and Somot (2008) concluded that the necessary resolution for atmospheric forcing in order to simulate Mediterranean convection and deep water formation is about 50 km. Therefore 'normal' deep water formation events are probably not reproduced by the ORCA025 simulations.

Mean sea level

Performance regarding sea level in the simulations is analysed by comparing them to altimetry over the available common period (1993-2004/2007/2009). Detailed comparison of mean sea level from altimetry and SSH from G70 can be found in Vidal-Vijande *et al.* (2011) and will not be repeated here. However, their main result in this regard was that the model was capable of correctly reproducing the seasonal cycle in both phase and amplitude as well as the interannual variability, but SSH from the model showed an exaggerated positive trend

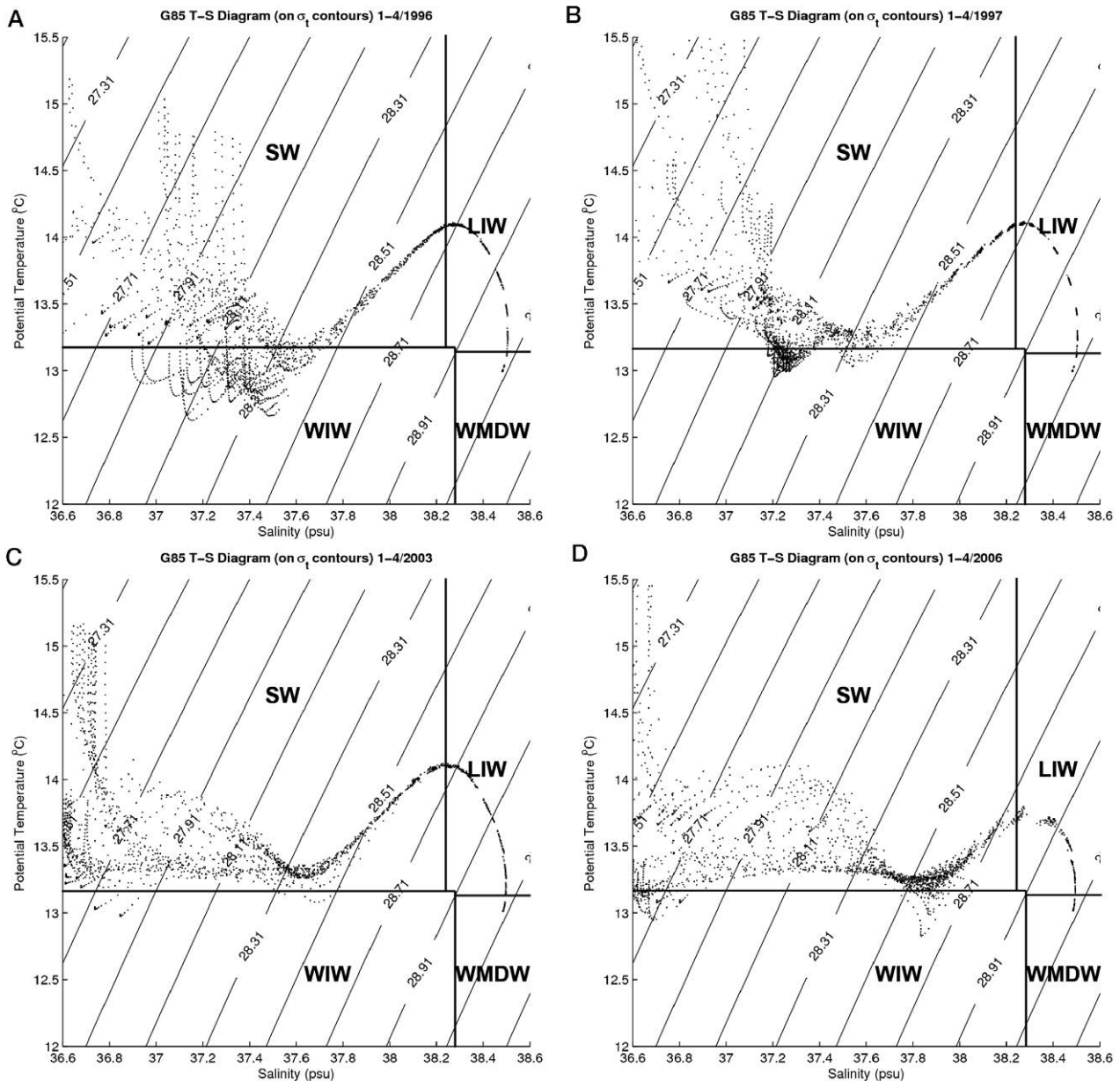


FIG. 10. – TS Diagrams of a $1^{\circ} \times 1^{\circ}$ area at the centre of the Ibiza Channel for the G85 simulation for the period January to April 1996 (A), 1997 (B), 2003 (C) and 2006 (D). SW stands for surface waters, the rest of the acronyms are detailed in the text.

of $14.96 \pm 1.46 \text{ mm yr}^{-1}$ when the trend for altimetry was $3.62 \pm 1.32 \text{ mm yr}^{-1}$. G85 also displays a correct seasonal cycle but the trend has increased even further to $20.27 \pm 1.37 \text{ mm yr}^{-1}$ due to the effect of a reduced salinity relaxation term, which implies lower evaporation and therefore an increase in sea level.

These positive trends of the ORCA models are not an isolated feature of the Mediterranean, but global due to an imbalanced freshwater budget. The freshwater budget is of vital importance because it contributes to the mean sea-level budget closure, impacting sea-level rise and density-driven circulation (Ferry *et al.* 2010), but its contributors (precipitation, evaporation, river run-off and glacier melt) have great uncertain-

ties, making it very difficult to achieve a balance. If the trends are removed, the power spectra of G85 and altimetry (not shown) are very similar in terms of peaks and energy. Essentially, both spectra have a marked annual cycle at 10–12 months and a less well-defined semi-annual peak, but if trends are not removed, higher energy is seen in G85 at lower frequencies.

In GLORYS, the net water budget is artificially set to zero in each time step. It thus becomes perfectly balanced and does not affect the mean sea level (MSL) of the model. The consequence is that any changes in MSL are due to the assimilated data provided by altimetry (Ferry *et al.* 2010). As a result, the comparison between GLORYS and altimetry data yields almost

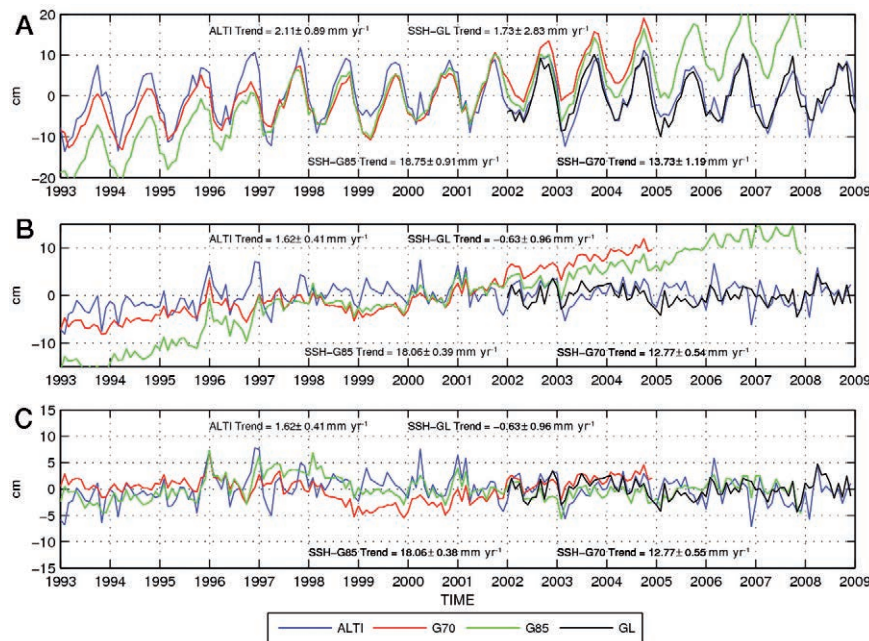


FIG. 11. – ORCA G70, G85 and GLORYS (GL, black) SSH plotted against altimetry mean sea-level anomaly for the WMED. (A) full signal (B) with the seasonal cycle removed (C) with seasonal cycle and trends removed (the numerical values indicate the trend that has been removed). A colour version of this figure may be found in the online electronic manuscript.

identical results, with no drift in the model's SSH and a trend very similar to altimetry

Mean circulation

We contrast the mean circulation of the G70 and G85 simulations with the available literature. The mean circulation in the WMED is well known. Atlantic waters go through the Strait of Gibraltar into the Alboran Sea (Astraldi *et al.* 1999, Beranger *et al.* 2005, Tsimplis and Bryden 2000, Sánchez-Román *et al.* 2009, García-Lafuente *et al.* 2002a, Gomis *et al.* 2006) and form the Western Alboran Gyre and the Eastern Alboran Gyre (Viúdez *et al.* 1998). The circulation continues out of the Alboran Sea as the Algerian Current (Millot 1999), which shows significant mesoscale activity as it continues towards the Sicily Channel. Part of it crosses the channel and the rest recirculates into the Tyrrhenian Sea, moving along the Italian Coast and becoming the Northern Current as it passes into the Ligurian, through the Gulf of Lions and into the Balearic Sea. The Northern Current recirculates before it reaches the Ibiza Channel and becomes the Balearic current (Pinot *et al.* 1995, Alvarez *et al.* 1994, Astraldi *et al.* 1999, Ruiz *et al.* 2009).

The ORCA models show the same general circulation pattern (Fig. 12). In more detail, both G70 and G85 show the presence of the Western and Eastern Alboran Gyres, with G70 showing a more prominent Western Alboran Gyre. Given the coarse resolution, both models aggregate the Algerian Current and the area of intense mesoscale activity above the Algerian Current into one meandering, high-intensity band, with G85

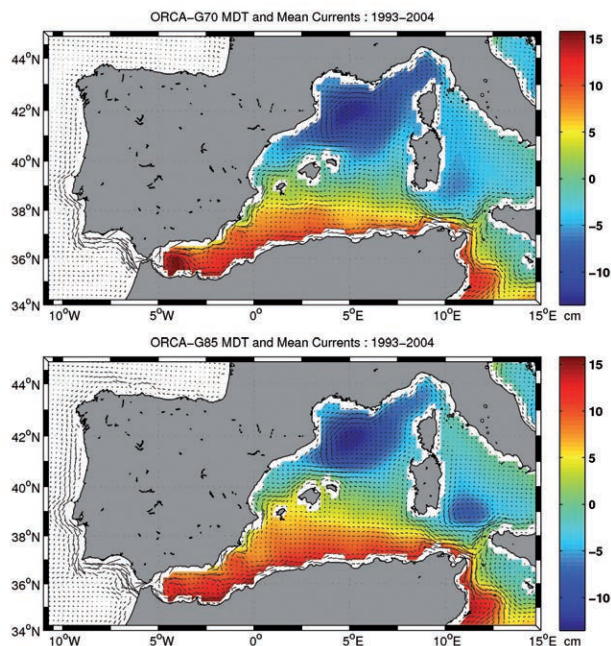


FIG. 12. – Mean Dynamic Topography (MDT) maps from G70 (top) and G85 (bottom) with surface velocity vectors added. A colour version of this figure may be found in the online electronic manuscript.

reaching further north than G70. Both models show low minima to the SE of the Gulf of Lions and between Sardinia and Sicily, with G70 being more intense in the former and G85 in the latter. In the Balearic Sea, G70 reproduces the recirculation of the Northern Current further south than G85, closer to the Ibiza Channel.

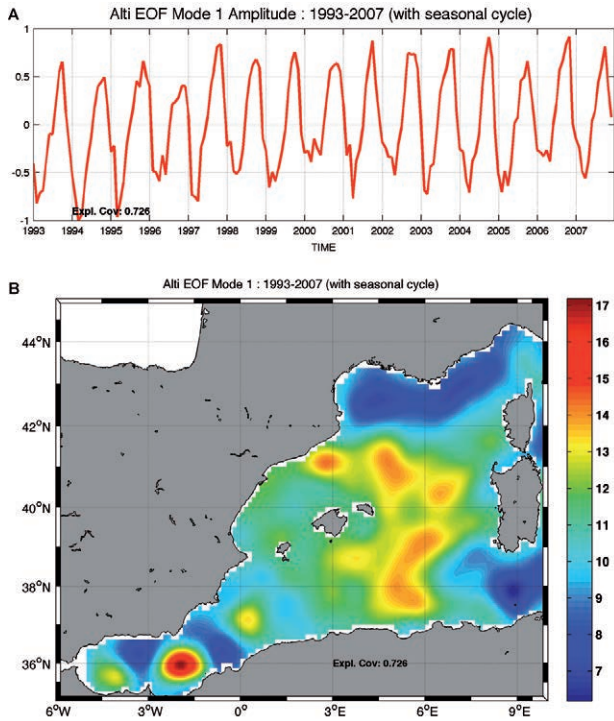


FIG. 13. – The first EOF mode for altimetry SLA (sea-level anomaly) with the amplitude (top) and pattern (bottom). A colour version of this figure may be found in the online electronic manuscript.

EOF analysis of SSH

We further evaluate the main patterns of variability of G85 by using empirical orthogonal functions (EOFs) and comparing with altimetry. Figures 13 and 14 present the first EOF mode of altimetry and G85 SSH respectively. The first EOF mode of altimetry, which explains 72.6% of the covariance, shows the strong seasonal variability of the Alboran Gyres with maximum amplitude in autumn (Larnicol *et al.* 2002). Also seen is the autumn/winter intensification of the cyclonic circulation in the Gulf of Lions. In the first EOF mode of G85 (86.2% coverage) the seasonality of the cyclonic gyre in the Gulf of Lions is also observed to a certain degree, but weaker and more towards the north. The signature of the Alboran anticyclonic gyres is almost negligible in G85. Along the path of the Algerian Current, G85 does not show the mesoscale variability seen in altimetry as expected, though it does exhibit a north-south gradient.

Figure 15 and 16 show the first EOF mode of both datasets with the seasonal cycle removed. As is to be expected, altimetry displays more intricate mesoscale patterns and better-defined eddy structures such as the Western Alboran Gyre and the Eastern Alboran Gyre. Despite the weaker Alboran gyres seen in G85 and the stronger pattern in the area of the Gulf of Lions, the simulation does show similar (but more diffuse) mesoscale patterns along the path of the Algerian Current, particularly the eddy east of the Almería-Orán front and the two eddies southeast of the Balearic Islands.

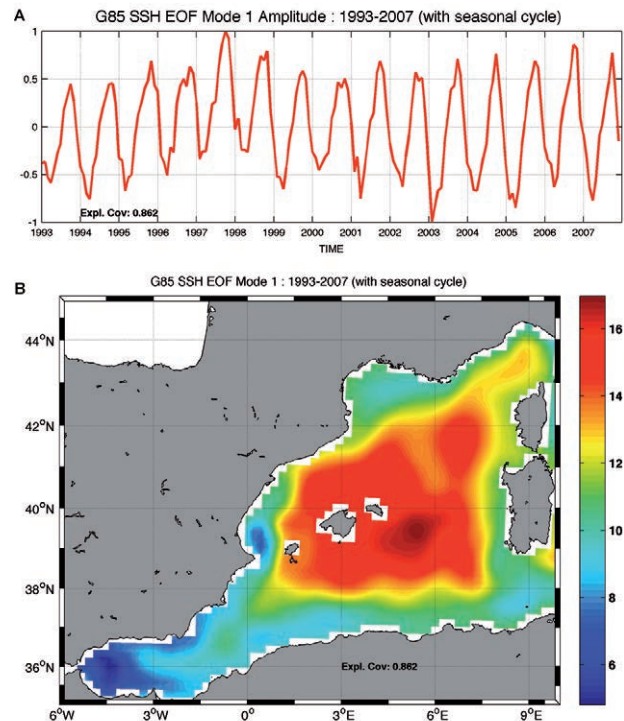


FIG. 14. – The first EOF mode for G85 SSH with the amplitude (top) and pattern (bottom). A colour version of this figure may be found in the online electronic manuscript.

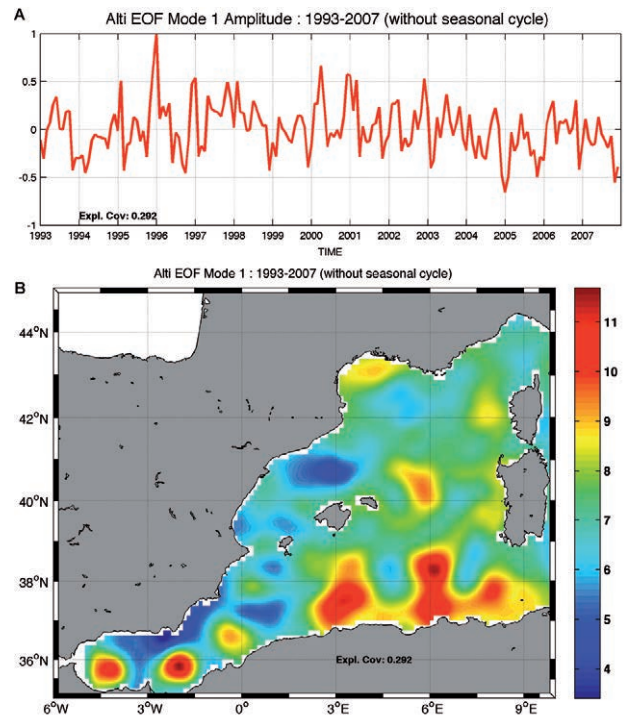


FIG. 15. – The first EOF mode for altimetry (without seasonal cycle) with the amplitude (top) and pattern (bottom). A colour version of this figure may be found in the online electronic manuscript.

The normalized amplitude time series of the first EOF mode show great disparities, although there are coincidences in the position of some peaks, such as 1996.

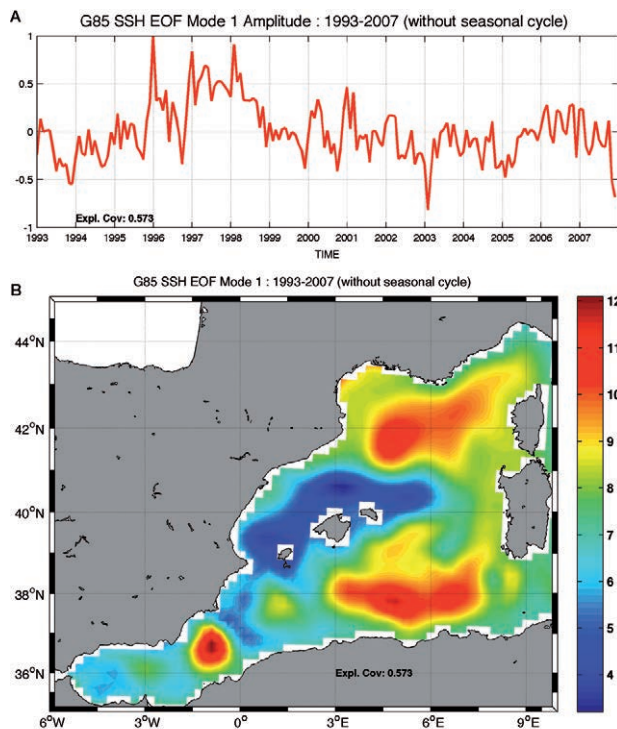


FIG. 16. – The first EOF mode for G85 SSH (without seasonal cycle) with the amplitude (top) and pattern (bottom). A colour version of this figure may be found in the online electronic manuscript.

The difference in the explained covariance of the two datasets can be attributed to resolution. In altimetry, subsequent modes (not shown) correspond mainly to marked mesoscale eddy features which the model has trouble resolving.

TRANSPORTS

Strait of Gibraltar

The only point of contact between the Mediterranean and the open ocean is the Strait of Gibraltar, which is therefore a key location to study because it is where the water balance of the Mediterranean is maintained. The correct representation of this transport is crucial for a model to work properly within the Mediterranean. Table 1 shows the transport values for the simulations analysed in this study. G70 has an inflow of 1.08 ± 0.08 Sv, an outflow of 1.01 ± 0.09 Sv and a net inflow of 0.07 ± 0.06 Sv. G85 has a slightly less intense exchange with 1.01 ± 0.09 Sv inflow, 0.95 ± 0.1 Sv outflow and a weaker 0.05 ± 0.06 Sv net inflow. GLORYS shows a more intense exchange (1.30 ± 0.12 Sv inflow, -1.24 ± 0.10 Sv outflow) but a similar net flow to G85 (0.05 ± 0.1 Sv). In this regard, all three models fall within the established observational values, which in themselves show great uncertainty because of the lack of long-term direct measurements, the complexity of a horizontal and vertical profile of the flow, and the presence of strong tidal currents (Tsimplis and Bryden 2000, Gomis *et al.* 2006).

TABLE 1. – Mean transport values through the Strait of Gibraltar from G70, G85 and GLORYS

	ORCA G70 (1993-2004)	ORCA G85 (1993-2007)	GLORYS (2002-2009)
IN	1.076 ± 0.08 Sv	1.006 ± 0.09 Sv	1.296 ± 0.12 Sv
OUT	1.008 ± 0.09 Sv	0.955 ± 0.10 Sv	1.243 ± 0.10 Sv
NET	0.067 ± 0.06 Sv	0.050 ± 0.06 Sv	0.052 ± 0.08 Sv

To date, no observational efforts have been maintained long enough to calculate a long-term mean. The longest study is by Soto-Navarro *et al.* (2010), who combined atmospheric data from reanalysis, satellite and experimental observations to calculate a four-year time series of the Atlantic inflow using the net flow estimated from the Mediterranean water budget and the Mediterranean outflow derived from current meter observations. They obtained a mean Atlantic inflow of 0.81 ± 0.06 Sv, a mean Mediterranean outflow of 0.78 ± 0.05 Sv and a net flow of 0.038 ± 0.007 Sv. Another study by Candela (2001), covering two years from October 1994 to October 1996 and using current profile measurements, obtained inflows of 1.01 Sv, outflows of 0.97 Sv and a net inflow of 0.04 Sv. Other studies by Tsimplis and Bryden (2000) and García Lafuente *et al.* (2002b) show weaker exchange and net flows but their studies were performed over periods of 4 and 6 months, respectively, so they did not capture a full year's cycle.

Ibiza and Mallorca Channels

The Ibiza Channel and the Mallorca Channel are passages where significant north-south water exchange in the WMED takes place (Fernández *et al.* 2005), Ibiza being the most important of the two with over twice the amount of flux. Across the Ibiza Channel transport shows a marked seasonal cycle, with maximum southward flow during winter months (January-March) and maximum northward flow in summer. In the Mallorca Channel, a seasonal cycle is also present but there is flow in both directions throughout the year. In this study we focus primarily on the Ibiza Channel, where both G70 and G85 (Fig. 17) display the appropriate north-south seasonal variability with similar flow values. G70 (not shown) shows mean northward transport of 0.63 ± 0.3 Sv, southward transport of 0.23 ± 0.14 Sv and a net northward transport of 0.40 ± 0.37 Sv. G85 has a mildly stronger northward transport of 0.72 ± 0.34 , a slightly more intense southward transport of 0.23 ± 0.23 Sv and a net northward transport of 0.49 ± 0.51 Sv. The associated error is a little higher in G85. By computing transport at different layers, it was determined that northward transport occurs in surface layers and southward transport occurs mainly in intermediate and deep layers.

GLORYS has a northward transport similar in magnitude to that of the other two models but its southward transport is far more intense, with an average of 0.67 ± 0.56 Sv, normal annual peaks of over 1 Sv and

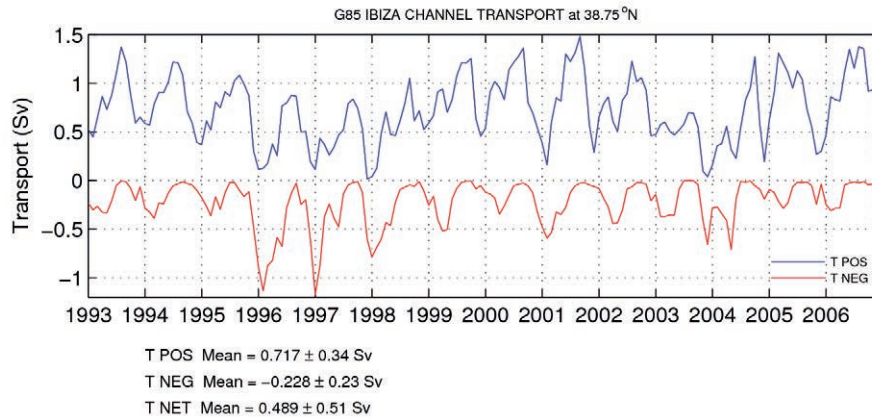


FIG. 17. – Transport time series for the G85 simulation in the Ibiza Channel for the period 1993-2007. Mean transport values are given below the figure. POS means flow in positive directions (north and east). NEG means flow in the negative directions (south and west). A colour version of this figure may be found in the online electronic manuscript.

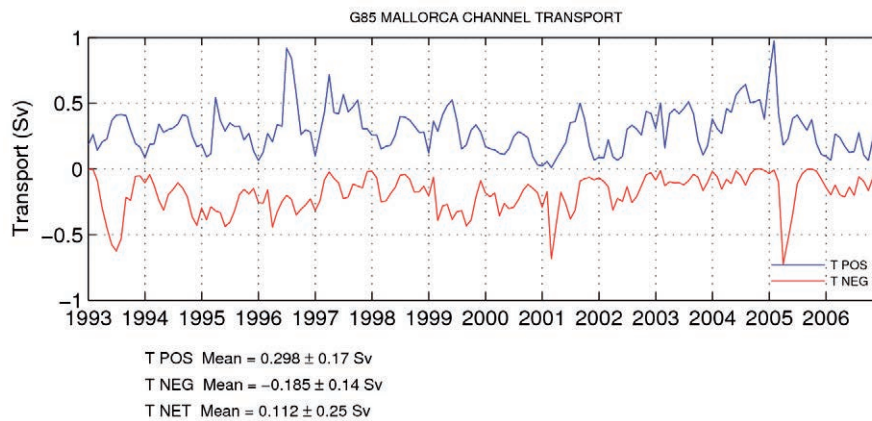


FIG. 18. – Transport time series for the G85 simulation in the Mallorca Channel for the period 1993-2007. Mean transport values are given below the figure. POS means flow in positive directions (north and east). NEG means flow in the negative directions (south and west). A colour version of this figure may be found in the online electronic manuscript.

intense peaks of 2-2.5 Sv (winters of 2007 to 2009). These intense peaks are far greater than those found in the literature. It must be noted that these peaks occur in the final years of the simulation, where no direct observational data has been published yet, and could very well be exceptional years.

Fernández *et al.* (2005) calculated transports through several transects, straits and channels, using data from the DieCAST $1/8^\circ$ numerical model. They obtained maximum southward transports of 0.9 Sv in winter and northward transports of 1-1.4 Sv in summer (with very little northward transport in winter). Their data agrees with both ORCA simulations although G70 does not reach the maximum 0.9 Sv of southward transport. GLORYS agrees in the northward flow but generally overshoots the measured 0.9 Sv.

One of the most exhaustive observational studies in the Balearic Sea was undertaken by Pinot *et al.* (2002) and consisted of two years of hydrography experiments (the CANALES experiment) from 1996 to 1998. These included several sampling techniques to measure the flow through the Mallorca and Ibiza Channels. They

provide very detailed transport measurements over the two-year period, which coincide reasonably well with G85 in both the magnitude of transports and some of the smaller-scale variability. In the simulations, the Ibiza Channel (Fig. 17) coincides better with the observational data than the Mallorca Channel (Fig. 18). Pinot *et al.* (2002) measured peaks of 1.05 Sv moving southward through the Ibiza Channel during the winter of 1996, falling to 0.5 Sv by spring and fully reversing by summer, with a northward flow of recent Atlantic Water. By the beginning of winter, the flow has reversed again with dominating southward flow from the Northern Current. 1997 begins with a similar pattern to that of the previous year (0.9 Sv) and shows a very sharp decline with the beginning of spring because of an eddy blocking the channel. G85 also displays this sharp decline but it is probably not due to an eddy because the model is not capable of reproducing eddies of this small size. G70 does show similar variability but its maximum southward transport values seem to be underestimated. This could be due to the reduced vertical resolution of G70, especially in the intermediate and

deeper layers where most of the southward transport through the Ibiza Channel takes place. This appears to indicate that vertical resolution of the simulations is an important element in correctly reproducing transports.

SUMMARY AND CONCLUSIONS

We have analysed the performance of three global numerical simulations, G70, G85 and GLORYS (with assimilation), building on the previous work by Vidal-Vijande *et al.* (2011) but focusing on the WMED. All three simulations are based on a similar $1/4^\circ$ NEMO (Madec 2008) code configuration on an ORCA grid. G70 and G85 are hindcasts of the past half century developed by the DRAKKAR Group (Barnier *et al.* 2007). They differ in vertical resolution (G70 has 46 vertical levels and G85 has 75), slightly different forcing based on ERA40 (G70 has DFS3 and G85 the improved DFS4) and intensity of the surface salinity restoring term, with G85 being six times weaker than G70. The salinity restoring term is applied in order to correct for drift in the freshwater balance of the simulations; it adds salt or evaporation where needed based on a climatology. GLORYS has a similar configuration to G70 but includes data assimilation and runs over the period 2002 to 2008.

Mean temperature variability is well reproduced at surface and intermediate layers although G70 shows trends at deep and intermediate layers that are larger than those obtained from observational databases. The improved continuity of the DFS4 atmospheric forcing together with a higher vertical resolution greatly improves these trends in G85. The combined effect of a more consistent atmospheric forcing (interfacing between the ERA40 and ECMWF in 2002), corrected fluxes and more realistic wind stress ($\sim 10\%$ stronger, Brodeau *et al.* 2010) together with the increased vertical resolution, which improves the vertical mixing coefficient, cause a marked improvement in the intermediate and deep layer trends.

Salinity is the most problematic variable. Neither the interannual variability nor the trends coincide well with observations. SSS relaxation obliterates interannual variability and the degree of restoring directly affects the salinity trend. This is evident in G85, which shows very strong negative trends in surface and especially intermediate layers. Salinity is directly affected by the atmospheric forcing and freshwater balance of the simulations. Further work improving the quality and resolution of atmospheric forcing is likely to improve salinity results.

The exceptional deep convection events in the NW Mediterranean of 2004-2005 and 2005-2006 (Schroeder *et al.* 2006, 2008a, 2010, Herrmann *et al.* 2010, Font *et al.* 2007, Smith *et al.* 2008) were analysed in more detail using the G85 and GLORYS simulations (G70 finishes in 2004), as well as their propagation towards the Balearic Channels. These channels are of vital importance as they are where many of the north-south

water and heat exchanges in the WMED take place. These two exceptional winters were characterized by extreme evaporation and heat loss in the Gulf of Lions area, leading to very strong deep convection events, which also modified the properties of the LIW. In G85, the strong convection and modification of LIW is clearly visible, with the 2005-2006 winter convection actually penetrating below the LIW into deep layers. However, the low resolution of the model and especially of the atmospheric forcing results in weaker convection events not penetrating the LIW. This causes the intermediate layers to heat up because, as evidenced by the years 2004-2006, the winter entrainment of colder waters plays a vital role in maintaining the temperature of the LIW close to the observations. GLORYS shows the strong convection event in the 2005-2006 winter, and because of the availability of daily resolution the convection is very clearly marked and isolated. This is backed by the EN3 results, which also show the deep convection in both winters, with 2005-2006 being the strongest. These results show that as long as the forcing conditions are strong enough, these simulations are capable of producing deep waters despite the low atmospheric forcing resolution. However, during normal convection conditions these models are not capable of propagating the convection into deep waters because of the low spatial resolution of both the model and the atmospheric forcing, which needs to be at least 50 km in order to allow the simulation of Mediterranean convection (Li *et al.* 2006, Herrmann and Somot 2008, Beranger *et al.* 2010).

Regarding sea level, all models correctly reproduce the seasonal cycle and interannual variability but because the simulations without assimilation (G70 and G85) do not maintain the freshwater balance and underestimate evaporation (Herrmann *et al.* 2008), they display exaggerated positive trends. G70 displays a trend of 14.96 ± 1.46 mm yr⁻¹ and G85 with a weaker SSS restoring shows a greater positive trend (20.27 ± 1.37 mm yr⁻¹), indicating that at present these simulations require the restoring term in order to keep trends within acceptable levels. GLORYS has its water balance artificially adjusted at each time step, so does not suffer this problem.

We have found that all simulations recreate the mean surface circulation correctly within their resolution limits, which prevents them from resolving the mesoscale although through EOF pattern analysis some larger mesoscale features are indeed reproduced. Transport through the Strait of Gibraltar is within the established observational estimates (Candela 2001, Tsimplis and Bryden 2000, García Lafuente *et al.* 2002a), showing correct inflow (G70: 1.078 Sv, G85: 1.006 Sv), outflow (G70: 1.008 Sv, G85: 0.955 Sv) and net values (G70: 0.067, G85: 0.050 Sv). Only GLORYS appears to have a more intense exchange (1.296 Sv in, 1.243 Sv out) but a correct net flow (0.052 Sv). The Ibiza and Mallorca channels play a vital role in the WMED as it is through these channels that a large part

of the north-south exchange of heat and water occurs. All simulations display the correct seasonal variability in the Ibiza Channel, with predominant southward transport in winter and northward transport in summer. G70 has correct mean values but does not reproduce the 1996-1998 high southward transport events. These events are reproduced by G85 and coincide with the observations by Pinot *et al.* (2002) during the CANALES experiment. It is important to note that according to G85, these years are exceptional. GLORYS produces very intense southward flow (1.5 to 2.5 Sv), far exceeding the other simulations. Observations are not available for the GLORYS years so they cannot be directly compared, but available observational data of previous years show weaker transports (0.6 to 1.3 Sv).

This study contributes to the improvement of the ORCA hierarchy of simulations and points out the strengths and weaknesses of these simulations in the Mediterranean Sea. Future studies will involve the use of higher-resolution simulations such as the recently available 1/12° version of the ORCA simulations, combining the simulation data with satellite data (SST and altimetry both gridded and along-track), drifters and hydrographic data (CTDs and gliders). The study will focus on the physical characterization of the Balearic Sea and the heat and water fluxes passing through that area, taking special note of fluxes through the Balearic Channels.

ACKNOWLEDGEMENTS

We would like to thank the DRAKKAR Group and MERCATOR-Océan for providing the simulations analysed in this study. The first author would like to give special thanks to the CSIC I3P PreDoc Grant Programme for financing his PhD thesis work, as well as to the MyOcean FP7 EU Project for making part of this study possible. The altimeter products were produced by SSALTO/DUACS and distributed by AVISO with support from CNES. We would also like to acknowledge the work by the Hadley Centre in creating the EN3 dataset.

REFERENCES

- Alvarez A., Tintoré J., Holloway G., Eby M., Beckers J.M. 1994. Effect of topographic stress on circulation in the western Mediterranean. *J. Geophys. Res.* 99: 16,053-16,064.
- Astraldi M., Balopoulos S., Candela J., Font J., Gacic M., Gasparini G. P., Manca B., Theocharis A., Tintoré J. 1999. The role of straits and channels in understanding the characteristics of Mediterranean circulation. *Prog. Oceanogr.* 44: 65-108.
- Barnier B., Madec G., Penduff T., Molines J.M., Treguier A.M., Sommer J.L., Beckmann A., Biastoch A., Böning C., Dengg J., Derval C., Durand E., Gulev S., Remy E., Talandier C., Theetten S., Maltrud M., McClean J., Cuevas B.D. 2006. Impact of partial steps and momentum advection schemes in a global ocean circulation model at eddy-permitting resolution. *Ocean Dyn.* 56: 543-567.
- Barnier B., Brodeau L., Le Sommer J., Molines J.M., Penduff T., Theetten S., Treguier A.M., Madec G., Biastoch A., Böning C., Dengg J., Gulev S., Badie B.R., Chanut J., Garric G., Alderson S., Coward A., de Cuevas B., New A., Haines K., Smith G., Drijfhout S., Hazeleger W., Severijns C., Myers P. 2007. Eddy-permitting ocean circulation hindcasts of past decades. *CLIVAR Exchanges* 42 (vol 12, number 3): 8-10
- Beranger K., Mortier L., Crepon M. 2005. Seasonal variability of water transport through the straits of Gibraltar, Sicily and Corsica, derived from a high-resolution model of the Mediterranean circulation. *Prog. Oceanogr.* 66: 341-364.
- Beranger K., Drillet Y., Houssais M.-N., Testor P., Bourdallé-Badie R., Alhammoud B., Bozec A., Mortier L., Bouruet-Aubertot P., Crepon M. 2010. Impact of the spatial distribution of the atmospheric forcing on water mass formation in the Mediterranean Sea. *J. Geophys. Res.* 115: C12041.
- Beuvier J., Sevault F., Herrmann M., Kontoyiannis H., Ludwig W., Rixen M., Stanev E., Béranger K., Somot S. 2010. Modeling the Mediterranean Sea interannual variability during 1961-2000: Focus on the eastern Mediterranean transient. *J. Geophys. Res.* 115: C08017.
- Brodeau L., Barnier B., Treguier A.M., Penduff T., Gulev S. 2009. An ERA40-based atmospheric forcing for global ocean circulation models. *Ocean Model.* 31: 88-104.
- Calafat F.M. 2010. *Quantification of the different contributions of long-term sea-level variability in the Mediterranean Sea*. PhD thesis, Univ. Illes Balears.
- Candela J. 2001. Mediterranean water and global circulation. In: Siedler G., Church J., Gould J. (eds.), *Ocean Circulation and Climate*. Academic Press, New York, pp. 419-429.
- Dobricic S. 2005. New mean dynamic topography of the Mediterranean calculated from assimilation system diagnostics. *Geophys. Res. Lett.* 32: L11606.
- Fernández V., Dietrich D.E., Haney R.L., Tintoré J. 2005. Mesoscale, seasonal and interannual variability in the Mediterranean Sea using a numerical ocean model. *Prog. Oceanogr.* 66: 321-340.
- Ferry N., Parent L., Garric G., Barnier B., Jourdain N.C., Mercator Ocean Team. 2010. Mercator global eddy permitting ocean reanalysis GLORYS1V1: Description and results. *Mercator Newsletter* 36: 15-27.
- Font J., Puig P., Salat J., Palanques A., Emelianov M. 2007. Sequence of hydrographic changes in NW Mediterranean deep water due to the exceptional winter of 2005. *Sci. Mar.* 71: 339-346.
- Gaillard F., Autret E., Thierry V., Galaup P. 2008. Quality control of large Argo datasets. *J. Atmos. Ocean. Tech.* 26: 337-351.
- Gaillard F., Charraudeau R. 2008. New climatology and statistics over the global ocean. MERSEA del 5.4.7, Ref. CNRS-STR-001, IFREMER, 9 pp.
- García-Lafuente J., Delgado J., Criado F. 2002a. Inflow interruption by meteorological forcing in the strait of Gibraltar. *Geophys. Res. Lett.* 29: 1914.
- García-Lafuente J., Delgado J., Vargas J.M., Vargas M., Plaza F., Sarhan T. 2002b. Low-frequency variability of the exchanged flows through the strait of Gibraltar during CANIGO. *Deep-Sea Res.* II 49: 4051-4067.
- Gomis D., Tsimplis M.N., Martín-Míguez B., Ratsimandresy A.W., García-Lafuente J., Josey S.A. 2006. Mediterranean sea level and barotropic flow through the strait of Gibraltar for the period 1958 – 2001 and reconstructed since 1659. *J. Geophys. Res.* 111: C11005.
- Goosse H. 1997. Modelling the large scale behaviour of the coupled ocean-ice system. PhD thesis, Université Catholique de Louvain, Louvain-la-Neuve, Belgium.
- Herrmann M., Somot S., Sevault F., Estournel C., Déqué M. 2008. Modeling the deep convection in the northwestern Mediterranean Sea using an eddy-permitting and an eddy-resolving model: Case study of winter 1986-1987. *J. Geophys. Res.* 113: C04011.
- Herrmann M., Sevault F., Beuvier J., Somot S. 2010. What induced the exceptional 2005 convection event in the northwestern Mediterranean basin? Answers from a modeling study. *J. Geophys. Res.* 115: C12051.
- Herrmann M.J., Somot S. 2008. Relevance of ERA40 dynamical downscaling for modeling deep convection in the Mediterranean Sea. *Geophys. Res. Lett.* 35: L04607.
- Ingleby B., Huddleston M. 2007. Quality control of ocean temperature and salinity profiles – historical and real-time data. *J. Mar. Syst.* 65: 158-175.
- Ishii M., Kimoto M. 2009. Reevaluation of historical ocean heat content variations with time-varying XBT and MBT depth bias corrections. *J. Oceanogr.* 65: 287-299.

- Kantha L.H., Clayson C. 2000. Numerical models of Oceans and Oceanic Processes. *Intl. Geophys. Series* 66. Academic Press, USA.
- Large W., Yeager S. 2004. Diurnal to decadal global forcing for ocean and sea-ice models; The Data Sets and Flux Climatologies. Technical Report, NCAR/TN-460+STR, NCAR.
- Larnicol G., Ayoub N., Le Traon P.Y. 2002. Major changes in Mediterranean Sea level variability from 7 years of TOPEX/Poseidon and ers-1/2 data. *J. Mar. Syst.* 33-34: 63-89.
- Lebeaupin Brossier C., Béranger K., Dêtel C., Drobinski P. 2011. The Mediterranean response to different space-time resolution atmospheric forcings using perpetual mode sensitivity simulations. *Ocean Model.* 36: 1-25.
- Li L., Bozec A., Somot S., Béranger K., Bouruet-Aubertot P., Sevault F., Crépon M. 2006. Regional atmospheric, marine processes and climate modelling. In: Lionello P., Boscolo R. (eds.), *Developments in Earth and Environmental Sciences*, vol. 4, Elsevier, pp. 373-397.
- López-Jurado J., Gonzalez-Pola C., Velez-Belchi P. 2005. Observation of an abrupt disruption of the long-term warming trend at the Balearic Sea, Western Mediterranean Sea, in summer 2005. *Geophys. Res. Lett.* 32: L24606.
- Madec G. 2008. NEMO ocean engine. Note du Pôle de modélisation, 27. ISSN No 1288-1619. IPSL/LODYC, Université P. et M. Curie, B102 T15-E5, 4 place Jussieu, Paris cedex 5, France.
- Madec G., Delecluse P., Imbard M., Levy C., 1998. OPA 8.1, Ocean general circulation model, reference manual. Notes du Pôle de modélisation. IPSL/LODYC, Université P. et M. Curie, B102 T15-E5, 4 place Jussieu, Paris cedex 5, France
- MEDAR-Group 2002. MEDATLAS/2002 database: Mediterranean and Black Sea database of temperature salinity and biochemical parameters, in Climatological Atlas [CD-ROM], Fr. Res. Inst. For Exploit. of Sea, Issy-les-Moulineaux, France.
- Millot C. 1999. Circulation in the western Mediterranean sea. *J. Mar. Syst.* 20: 423-442.
- Molines J.M., Barnier B., Penduff T., Brodeau L., Treguier A., Theetten S., Madec G. 2007. Definition of the interannual experiment ORCA025-G70, 1958-2004. Report LEGI-DRA-2-11- 2006i, LEGI.
- Penduff T., Juza M., Barnier B. 2007. Assessing the realism of ocean simulations against hydrography and altimetry. *CLIVAR Exchanges* 12(3): 11-12.
- Pinot J.M., Tintoré J., Gomis D. 1995. Multivariate analysis of the surface circulation in the Balearic Sea. *Progr. Oceanogr.* 36: 343-344.
- Pinot J.M., López-Jurado J.L., Riera M. 2002. The CANALES Experiment (1996-1998). interannual, seasonal, and mesoscale variability of the circulation in the Balearic channels. *Progr. Oceanogr.* 55: 335-370.
- Pujol M.-I., Larnicol G. 2005. Mediterranean sea eddy kinetic energy variability from 11 years of altimetric data. *J. Mar. Syst.* 58:121-142.
- Rixen M., Beckers J.M., Levitus S., Antonov J., Boyer T., Maillard C., Fichaut M., Balopoulos E., Iona S., Dooley H., Garcia M.J., Manca B., Giorgetti A., Manzella G., Mikhailov N., Pinardi N., Zavatarelli M. 2005. The Western Mediterranean Deep Water: A proxy for climate change. *Geophys. Res. Lett.* 32: L12608.
- Ruiz S., Pascual A., Garau B., Faugere Y., Alvarez A., Tintoré J. 2009. Mesoscale dynamics of the Balearic front, integrating glider, ship and satellite data. *J. Mar. Syst.* 78: S3-S16
- Sánchez-Román A., Sannino G., García-Lafuente J., Carillo A., Criado-Aldeanueva F. 2009. Transport estimates at the western section of the Strait of Gibraltar: A combined experimental and numerical modeling study. *J. Geophys. Res.* 114: C06002.
- Schroeder K., Gasparini G.P., Tangherlini M., Astraldi M. 2006. Deep and intermediate water in the western Mediterranean under the influence of the eastern Mediterranean transient. *Geophys. Res. Lett.* 33: L21607.
- Schroeder K., Ribotti A., Borghini M., Sorgente R., Perilli A., Gasparini G.P. 2008a. An extensive western Mediterranean deep water renewal between 2004 and 2006. *Geophys. Res. Lett.* 35: L18605.
- Schroeder K., Taillandier V., Vetrano A., Gasparini G. 2008b. The circulation of the western Mediterranean sea in spring 2005 as inferred from observations and from model outputs. *Deep-Sea Res. I* 55: 947-965.
- Schroeder K., Josey S.A., Herrmann M., Grignon L., Gasparini G.P., Bryden H.L. 2010. Abrupt warming and salting of the western Mediterranean deep water after 2005: Atmospheric forcings and lateral advection. *J. Geophys. Res.* 115: C08029.
- Sevault F., Somot S., Beuvier J. 2009. A regional version of the NEMO Ocean Engine on the Mediterranean Sea: *NEMOMED8 user's guide*. Groupe de Météorologie de Grande Echelle et Climat, CNRM, Toulouse, France, note de Centre, 107.
- Simmons A., Gibson J. 2000. The ERA40 project plan. Technical Report 1, *European Centre for Medium Range Weather Forecast*, Reading, UK.
- Smith R., Bryden H.L., Stansfield K. 2008. Observations of new western Mediterranean deep water formation using Argo floats 2004-2006. *Ocean Sci.* 4: 133-149.
- Somot S., Sevault F., Déqué M. 2006. Transient climate change scenario simulation of the Mediterranean sea for the twenty-first century using a high-resolution ocean circulation model. *Climate Dyn.* 27: 851-879.
- Soto-Navarro, J., Criado-Aldeanueva F., García-Lafuente J., Sánchez-Román A. 2010. Estimation of the Atlantic inflow through the Strait of Gibraltar from climatological and *in situ* data. *J. Geophys. Res.* 115: C10023.
- Tonani M., Pinardi N., Dobricic S., Pujol I., Fratianni C. 2008. A high-resolution free-surface model of the Mediterranean sea. *Ocean Sci.* 4: 1-14.
- Tsimplis M.N., Bryden H.L. 2000. Estimation of the transports through the Strait of Gibraltar. *Deep-Sea Res. I* 47: 2219-2242.
- Tsimplis M.N., Marcos M., Somot S., Barnier B. 2008. Sea level forcing in the Mediterranean sea between 1960 and 2000. *Global Planet. Change* 63: 325-332.
- Tsimplis M.N., Marcos M., Colin J., Somot S., Pascual A., Shaw A. 2009. Sea level variability in the Mediterranean sea during the 1990s on the basis of two 2d and one 3d model. *J. Mar. Syst.* 78: 109-123.
- Vidal-Vijande E., Pascual A., Barnier B., Molines J.M., Tintoré J. 2011. Analysis of a 44-year hindcast for the Mediterranean Sea: comparison with altimetry and *in situ* observations. *Sci. Mar.* 75: 71-86
- Viúdez A., Pinot J. M., Haney R.L. 1998. On the upper layer circulation in the Alboran Sea. *J. Geophys. Res.* 103: 21653-21666.

Received February 28, 2011. Accepted January 13, 2012.
Published online August 5, 2012.